Carrier-carrier scattering in photoexcited intrinsic GaAs quantum wells and its effect on femtosecond plasma thermalization

Martin Moško, Antónia Mošková, and Vladimír Cambel
Institute of Electrical Engineering, Slovak Academy of Sciences, Dúbravská cesta 9, SK-842 39 Bratislava, Slovakia
(Received 13 September 1994; revised manuscript received 9 January 1995)

When a nonthermal electron-hole plasma is excited close to the band edge of the intrinsic GaAs quantum well by a short laser pulse, the plasma thermalization occurs within about 200 fs [Knox *et al.*, Phys. Rev. Lett. **56**, 1191 (1986)]. According to previous Monte Carlo simulations, this fast process is due to carrier-carrier (*c-c*) scattering. Our work finds that *c-c* scattering causes much slower thermalization than the observed one. This conclusion is drawn from the Monte Carlo simulation with revised *c-c* scattering rates as well as from the molecular-dynamics simulation of many-body Coulomb kinetics, and the problem of explaining the rapid thermalization thus reappears. The *c-c* scattering rates derived by us are four times smaller than those used in previous simulations. In contrast to similar studies of bulk semiconductors we find a remarkably faster thermalization in the Monte Carlo simulation than in the molecular-dynamics simulation. The effect is ascribed to the breakdown of the Born-approximation treatment of binary collisions in the Monte Carlo method.

I. INTRODUCTION

Femtosecond laser pump-probe measurements reveal[1–3] that a nonthermal electron-hole (*e-h*) plasma excited close to the band edge of an intrinsic GaAs quantum well by a short laser pulse is thermalized within about 200 fs. This was shown[1] for the photoexcited *e-h* pair density $N_s = 2 \times 10^{10}\text{cm}^{-2}$. Since the carriers were excited with energies below the threshold for optical phonon emission, the 200 fs thermalization was ascribed to carrier-carrier scattering, in agreement with Monte Carlo (MC) simulations.[4–7] This work examines the experiment[1] by a MC simulation with revised carrier-carrier scattering rates as well as by the molecular dynamics (MD) simulation of classical many-body Coulomb kinetics. We find that the thermalization due to carrier-carrier scattering is much slower than the observed one.

In Sec. II, our MC and MD techniques for two-dimensional (2D) carrier-carrier scattering are discussed. The carrier-carrier scattering rates derived by us are four times smaller than those used in the MC simulations that fit the pump-probe measurements.[1] Exchange is included within a multisubband model. MD simulation of classical many-body Coulomb interactions in the 2D *e-h* plasma is described including details of implementation.

In Sec. III, the calculations of the thermalization of a low-density 2D *e-h* plasma are presented for the experimental conditions of Ref. 1. The agreement of the previous MC simulations with experiment is found to be fortuitous, because the MC simulation with our revised (four times smaller) carrier-carrier scattering rates gives two-to-three times slower thermalization than the observed one. In the revised MC simulation the thermalization is still overestimated, because the Born approximation is found to overestimate the exact quantum differential cross section for carrier-carrier scattering. The classical MD simulation shows much slower thermalization than the MC, because the classical differential cross section for carrier-carrier scattering is close to the exact one.

In Sec. IV, a summary is given. Unlike the previous interpretations[1–7] our MC and MD calculations do not confirm that the 200 fs thermalization in intrinsic GaAs quantum wells[1,3] is due to carrier-carrier scattering, although such an interpretation is invoked by physical intuition. We believe that a quantitative microscopic explanation of the 200 fs thermalization mechanism is still missing.

II. SIMULATION TECHNIQUES FOR CARRIER-CARRIER INTERACTIONS

First we reexamine the derivation of 2D *e-e* scattering rates, as pioneered in Ref. 8 and reviewed in Ref. 9. An electron changes its in-plane wave vector from $\mathbf{k}$ to $\mathbf{k}'$ and its subband quantum number from i to l by collision with another electron, which is scattered from the state $\mathbf{k}_0, j$ to the state $\mathbf{k}_0', n$. In the Born approximation, the total electron scattering rate from the state $\mathbf{k}, i$ into a final state in subband l is [see formula (2.17) in Ref. 8, with e^2 replaced by $e^2/4\pi$ in SI units]

$$\Gamma_{il}(\mathbf{k}) = \frac{e^4}{8\pi\hbar K^2 A} \sum_{j,n,\mathbf{k}_0,s_0} f_j(\mathbf{k}_0) \int d\mathbf{k}_0' \frac{|F_{ijln}(Q)|^2}{Q^2 \epsilon(Q)^2} \times \delta\left(\frac{\hbar^2}{2m_e}[k^2 + k_0^2 - k'^2 - k_0'^2] + E_i + E_j - E_l - E_n \right), \quad (1)$$

where $\mathbf{k}' = \mathbf{k} + \mathbf{k}_0 - \mathbf{k}_0'$, $\mathbf{Q} \equiv \mathbf{k} - \mathbf{k}'$, E_i is the subband energy, m_e is the electron effective mass, K is the material permittivity, A is the area of the 2D gas, $\epsilon(Q)$ is the static screening function,[9] $F_{ijln}(Q)$ is the form factor,[8,9] and $f_j(\mathbf{k}_0)$ is the occupation number in subband j. For each $\mathbf{k}_0$ in (1) one should sum over two spin indices s_0.

Introducing the vectors

$$\mathbf{g} = \mathbf{k}_0 - \mathbf{k} \quad , \quad \mathbf{g}' = \mathbf{k}_0' - \mathbf{k}' \tag{2}$$

we have

$$\mathbf{Q} = \frac{\mathbf{g} - \mathbf{g}'}{2} \quad , \quad k^2 + k_0^2 - k'^2 - k_0'^2 = \frac{g^2 - g'^2}{2} \quad . \tag{3}$$

Using (2) and $\mathbf{k}' = \mathbf{k} + \mathbf{k}_0 - \mathbf{k}_0'$ we find $dk_{0x}' = \frac{1}{2}dg_x'$, $dk_{0y}' = \frac{1}{2}dg_y'$, i.e.,

$$d\mathbf{k}_0' = \frac{1}{4}d\mathbf{g}' \quad , \tag{4}$$

where $d\mathbf{k}_0' \equiv dk_{0x}'dk_{0y}'$ and $d\mathbf{g}' \equiv dg_x'dg_y'$. When (3) and (4) are used in (1), the integral over g' gives

$$\Gamma_{il}(\mathbf{k}) = \frac{e^4 m_e}{16\pi\hbar^3 K^2 A} \sum_{j,n,\mathbf{k}_0,s_0} f_j(\mathbf{k}_0) \times \int_0^{2\pi} d\theta \frac{|\, F_{ijln}(Q)\,|^2}{Q^2\epsilon(Q)^2} \quad , \tag{5}$$

where θ is the angle between $\mathbf{g}$ and $\mathbf{g}'$,

$$Q = \frac{1}{2}[2g^2 + g_0^2 - 2g(g^2 + g_0^2)^{1/2}\cos\theta]^{1/2} \quad , \tag{6}$$

and g_0^2 is $4m_e(E_i + E_j - E_l - E_n)/\hbar^2$. The e-e scattering rate (5) is *four times smaller* than that derived in Refs. 8 [formula (2.21)] and 9, where the factor of 1/4 is missing in the substitution (4). The same problem is involved in the e-h scattering rate,[6,9] which can be obtained correctly from (5) by replacing m_e in (5) and (6) by the reduced effective mass $\mu = 2m_e m_h/(m_e + m_h)$ and taking $\mathbf{g}$ and $\mathbf{g}'$ as

$$\mathbf{g} = \mu\left(\frac{\mathbf{k}_0}{m_h} - \frac{\mathbf{k}}{m_e}\right) \quad , \quad \mathbf{g}' = \mu\left(\frac{\mathbf{k}_0'}{m_h} - \frac{\mathbf{k}'}{m_e}\right) \quad . \tag{7}$$

(Here m_h is the hole effective mass.) The factor of 1/4 is missing in previous calculations[4–11] including ours.[12–15] In the 3D case one finds $d\mathbf{k}_0' = \frac{1}{8}d\mathbf{g}'$ instead of (4). We stress that the factor of 1/8 is not missing in the 3D e-e scattering rate derived in Ref. 16.

The scattering rate (5) does not include the exchange effect between the electrons of like spin. For $i = j = l = n$ (intrasubband scattering) the exchange has been included in our previous work.[13,14] A straightforward generalization for an arbitrary i, j, l, n in (5) requires the replacement

$$\frac{|\, F_{ijln}(Q)\,|^2}{Q^2\epsilon(Q)^2} \to \frac{1}{2}\left[\frac{|\, F_{ijln}(Q)\,|^2}{Q^2\epsilon(Q)^2} + \frac{|\, F_{ijnl}(Q')\,|^2}{Q'^2\epsilon(Q')^2} - \frac{F_{ijln}(Q)F_{ijnl}(Q')}{Q\epsilon(Q)Q'\epsilon(Q')}\right] \quad , \tag{8}$$

where

$$Q' = \frac{1}{2}[2g^2 + g_0^2 + 2g(g^2 + g_0^2)^{1/2}\cos\theta]^{1/2} \tag{9}$$

and $\mathbf{Q}' \equiv \mathbf{k} - \mathbf{k}_0' = (\mathbf{g} + \mathbf{g}')/2$. The same scattering rates (with m_h instead of m_e) are valid for h-h scattering. In the case of intrasubband scattering $g_0 = 0$ and we have[13]

$$Q = g\,\sin\frac{\theta}{2} \quad , \quad Q' = g\left|\cos\frac{\theta}{2}\right| \quad . \tag{10}$$

We use the MC algorithm as discussed previously,[13] except that now the above mentioned factor of 1/4 is not missing in the carrier-carrier scattering rates. Carrier scattering by bulk polar optical phonons at a lattice temperature of 300 K is also considered. Photoexcited electrons and heavy holes are assumed to occupy only the lowest subband of the 10 nm GaAs quantum well,[1] while the occupation of higher subbands (including light-hole subbands) can be neglected.[3,5,6] The form factor $F_{1111}(Q)$ is calculated for both types of carriers using a sine envelope function. In this simple case, the static screening function can be expressed as[13]

$$\epsilon(Q) = 1 + \frac{Q_{sc}}{Q}F_{1111}(Q) \quad , \qquad Q_{sc} = \frac{e^2}{2\pi K\hbar^2}\left[m_e f_1^e(0) + m_h f_1^h(0)\right] \quad , \tag{11}$$

where $f_1^e(0)$ and $f_1^h(0)$ are the electron and hole occupation numbers at the bottom of the subband. $\epsilon(Q)$ is recalculated during the thermalization after each 5 fs,[13] because $f_1(0)$ varies in time. Adopting a *quasidynamic screening model*[13,17] we introduce the dynamic screening into the simulation as follows. In the case when $\epsilon(Q)$ screens the e-e interaction, the term $m_h f_1^h(0)$ in (11) is omitted. This approximate model is based on the assumption that heavy holes are too slow to follow the fast changes of electron positions and do not contribute to the dynamic screening of the e-e interaction.

To include dynamic screening and to treat carrier-carrier collisions like continuous many-body events, MD simulations of carrier thermalization have been developed for quantum wires,[18] quantum wells,[15,19] and bulk semiconductors.[17,20] Our MD simulates the perfectly 2D e-h plasma with free motion in the x and y directions. The dynamics of the ith carrier is governed by the Newton equations $\dot{\mathbf{k}}_i = \mathbf{F}_i/\hbar$, $\dot{\mathbf{r}}_i = \hbar\mathbf{k}_i/m_i$, where

$$\mathbf{F}_i = \sum_j -\frac{q_i q_j}{4\pi K}\frac{(\mathbf{r}_i - \mathbf{r}_j)}{|\,\mathbf{r}_i - \mathbf{r}_j\,|^3} \tag{12}$$

is the Coulomb force due to all other carriers. The Newton equations are solved by a finite difference method[18,21] with a time step Δt and $\mathbf{F}_i$ is recalculated after each step. The time step $\Delta t = 0.1$ fs is small enough to have an accurate simulation of the system.[22] As for the boundary conditions, we define a basic square cell of area L^2, which contains N carriers [$L^2 = N/(2N_s)$, $N = 5000$]. When a carrier leaves the cell crossing the boundary $x = L$, another carrier is injected into the cell at the equivalent boundary $x = 0$ with the same values of $\mathbf{k}$ and y. A similar reinjection is used at $x = L$ when a carrier leaves across the boundary $x = 0$ and an analogous convention is adopted at the boundaries $y = 0$ and $y = L$. Thus an infinite system is simulated using finite and constant

N. To calculate the Coulomb force (12) for an infinite system a carrier should be considered to interact with all other carriers in the cell and also with all carrier images in the periodic replicas of the cell. Such an Ewald sum calculation is time consuming. In Ref. 23 the minimum image approximation for the Ewald sum has been found to work well for plasma coupling constant Γ as large as 36. In our case Γ is typically 100 times smaller, i.e., the minimum image approximation is even more reliable. In this approximation a carrier interacts only with $N-1$ carriers in the cell through specially defined intercarrier distances. The calculated value of $x_i - x_j$ is used in the sum (12) only if $\mid x_i - x_j \mid \leq L/2$. If $x_i - x_j > L/2$, then $x_i - x_j$ is replaced in (12) by $x_i - x_j - L$. If $x_i - x_j < -L/2$, then $x_i - x_j$ is replaced in (12) by $x_i - x_j + L$. The same convention is adopted for $y_i - y_j$. The carrier at which the force is calculated is at the center of its own cell and the boundaries have no effect on the results.[24] Finally, our MD simulation is coupled with the MC simulation of carrier-phonon scattering.

In our simulations, photoexcited electrons and holes start their motion from Gaussian energy distributions of widths 17.4 meV and 2.6 meV, centered at 17.4 meV and 2.6 meV above the bottom of the first electron and hole subbands, respectively. Both distributions follow the energy spectrum of the laser pump pulse,[1] but the finite duration [100 fs (Ref. 1)] of the excitation is ignored. As discussed in Sec. III, empirical modeling of this effect would change our results insignificantly.

In our MD simulation, three initialization techniques were tested in order to isolate the effect of initial carrier positions on the thermalization. First, $\mathbf{r}(t=0)$ was selected for each carrier at random in the basic cell. Due to the repulsion of those electrons (holes) which were accidentally very close, the total kinetic energy weakly increased at the very beginning of the thermalization. A bound e-h state might also appear, when a too small e-h separation was accidentally selected. To suppress these effects we introduced a supplementing condition that the generation of two carriers closer than a certain distance is prohibited. Our second initialization technique suppresses these effects by generating a rather more homogeneous spatial distribution of carriers. The basic cell was divided into $N/2$ square subcells of area $L^2/(N/2)$ and one e-h pair was generated in each subcell with randomly chosen positions of both particles. Third, following Ref. 20, e-h pairs were introduced into the basic cell at random positions, with a fixed e-h separation that is small compared with the mean interparticle distance. In addition to the excess photon energy, a kinetic energy necessary to ionize the e-h pair was supplied. Electrons and holes need a few tens of femtoseconds to become ionized and to reach the Gaussian energy distributions mentioned above. Except for this feature, all three initializations give essentially the same evolution of the system and the relaxation in real space has a minor effect on the relaxation in $\mathbf{k}$ space.[25] Below we present the MD results obtained by the second initialization technique. This provides an appropriate comparison with the MC results (the MC simulation includes neither the relaxation in real space nor the ionization effect).

III. NUMERICAL RESULTS AND DISCUSSION

We start with the MC simulation, which treats the e-e, h-h, and e-h scattering within the quasidynamic screening model. The MC time step is 5 fs and the number of simulated e-h pairs is 20 000. The material parameters used in this paper are the same as previously.[12–15] The only difference is that the material permittivity K is now taken as the high-frequency permittivity ($10.9\epsilon_0$), not as the static one ($13\epsilon_0$). This is correct also for a statically screened carrier-carrier interaction.[26] The use of static permittivity decreases the carrier-carrier scattering rates about $(13/10.9)^2$ times.

Figure 1 shows the occupation numbers $f_1^e(\varepsilon_e)$ and $f_1^h(\varepsilon_h)$ vs electron energy ε_e and hole energy ε_h, respectively, at various times after the photoexcitation. Solid (dashed) curves are obtained using the e-e and h-h scattering rates without (with) exchange. As expected at low densities,[13] the thermalization with and without exchange is almost the same. In previous simulations,[6–9] the exchange has been approximately included into the e-e and h-h scattering rates by omitting the scattering between the carriers of like spin. This approximation would decrease the e-e and h-h scattering rates twice, so the thermalization of the dashed distributions in Fig. 1 would be slowed down almost twice. [In fact, in Refs. 4–9 this decrease was canceled by an artificial "partner carrier" scattering (p. 208 in Ref. 9), which has been shown[12] to increase the carrier-carrier scattering rates twice.]

Figure 2(a) shows differential transmission spectra $f_1^e[\varepsilon_e(k)] + f_1^h[\varepsilon_h(k)]$ vs excess photon energy $\varepsilon_e(k) + \varepsilon_h(k)$, obtained from the solid curves in Fig. 1. The initial nonthermal peak disappears at about 250 fs and the Maxwell-like distribution appears later than at 400

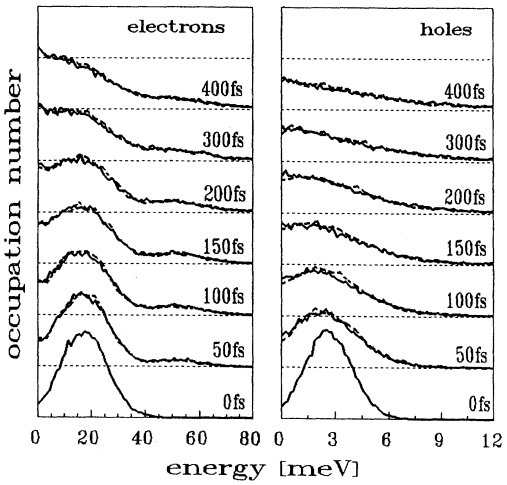

FIG. 1. Carrier occupation number vs carrier energy at times $0, 50, \ldots, 400$ fs after the photoexcitation. MC simulation includes the e-e, h-h, e-h, and carrier-phonon scattering at 300 K. The quasidynamic screening model is assumed. Solid (dashed) curves are obtained neglecting (including) the exchange. The distance between the horizontal grid lines is 0.02.

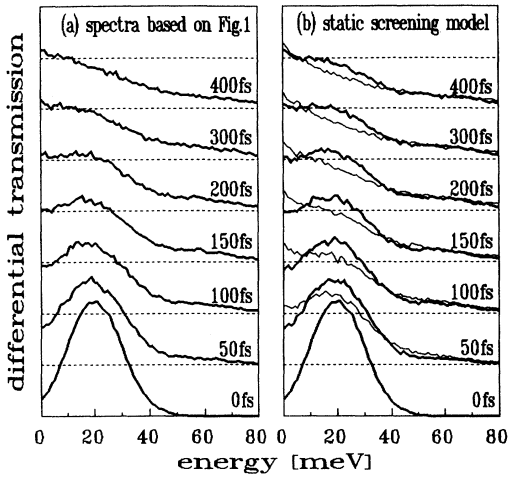

FIG. 2. Differential transmission vs excess photon energy. (a) Results obtained from the solid curves in Fig. 1. (b) Results based on the model that involves the static screening (11) with $F_{1111} = 1$ and neglects the exchange (thin solid curves are obtained by increasing carrier-carrier scattering rates by a factor of 4). The distance between the horizontal grid lines is 0.03.

fs. This is not in agreement with experiment (in the experiment[1] the nonthermal peak disappears at 100 fs and thermalization is completed at 200 fs).

In Fig. 2(b) we show the results based on the MC model, which includes the static screening function (11) with $F_{1111} = 1$ in e-e, e-h, and h-h interactions, and ignores the exchange. Due to static screening, the thick solid curves in Fig. 2(b) show rather slower thermalization than those in Fig. 2(a) (the nonthermal peak now disappears at 300 fs). The thin solid curves in Fig. 2(b), obtained with the carrier-carrier scattering rates artificially increased by a factor of 4, show a thermalized peak at 100 fs. They relax faster than in Ref. 6, where the same static screening model and the carrier-carrier scattering rates increased by a factor of 4 were used. This difference is mainly due to the fact that our Coulomb interaction contains the high-frequency permittivity instead of the static one and our form factor $F_{1111}(Q)$ is rather overestimated (due to the use of the sine envelope function). If the same model as in Ref. 6 were used without overestimating the carrier-carrier scattering rate by a factor of 4, our main MC results [Figs. 1 and 2(a)] would show even slower thermalization and larger disagreement with experiment.[1] The fortuitous agreement with experiment was likely the reason why the four-times-increased carrier-carrier scattering rates were used in Refs. 6, 7, and 9 without recognizing the overestimation.

We claimed in Ref. 15 that the scattering cross sections in the MC simulation are too large (two orders of magnitude larger than the mean intercarrier distance) for a binary collision model to be physically justified. This intuitive argument might seem to be weak due to the agreement between the MC results and experiment.[1] Now it is clear that the scattering cross sections were four times overestimated, but our MC model with revised carrier-carrier scattering does not fit the experiment.

In the experiment,[1] the peak of the pump laser pulse is centered at $t = 0$ with a 100 fs spread. An empirical model of this effect has been involved in previous MC simulations.[6,7,9] Since the agreement of these simulations with experiment has been achieved using four-times-overestimated carrier-carrier scattering rates, such an empirical model (instead of our instantaneous photoexcitation) cannot remove the disagreement between the experiment and MC simulation with revised scattering rates (Fig. 2). We keep the instantaneous photoexcitation in order to have a more transparent comparison of the MC and MD models.

Now we compare the plasma thermalization in the MC and MD simulations. Since our MD simulates Coulomb interactions of the perfectly 2D plasma, we now adopt the same approximation in the MC simulation in order to have a reliable comparative study. Assuming a δ-shaped envelope function we have $F_{1111} = 1$ in the e-e, e-h, and h-h scattering rates. The exchange effect is neglected and quasidynamic screening is considered in the screening function (11) (as already shown in Fig. 2, static screening only gives rather slower thermalization in our low-density case). Figure 3 shows the evolution of the electron and hole occupation numbers after the photoexcitation. The MD results (circles) show a much slower thermalization than the MC results (solid curves). This is an opposite trend when compared with bulk simulations.[17] Another surprising feature of our MD results is that the hole thermalization is slower than the electron thermalization. MC results show a faster thermalization for holes than for electrons, as already pointed out in Refs. 6 and 9. Figure 4 shows the transmission spectra based on Fig. 3. The MC spectra resemble the electron distribution

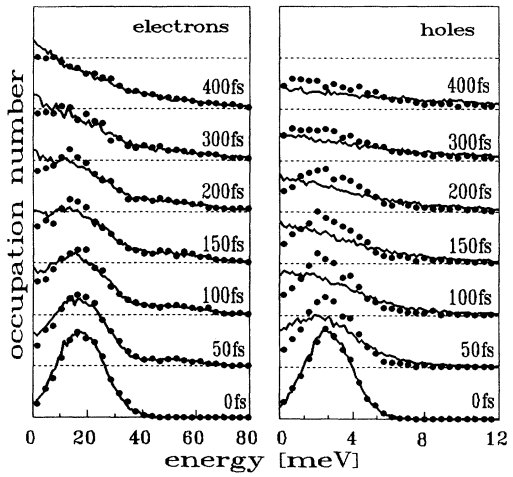

FIG. 3. Carrier occupation number vs carrier energy at times $0, 50, \ldots, 400$ fs after the photoexcitation. Solid curves and circles are obtained by the MC and MD simulations, respectively. MC simulation is the same as described in Fig. 1, except that a δ-shaped envelope function is now used in the carrier-carrier scattering rates. The carrier-phonon scattering at 300 K is included also in the MD simulation. The distance between the horizontal grid lines is 0.02.

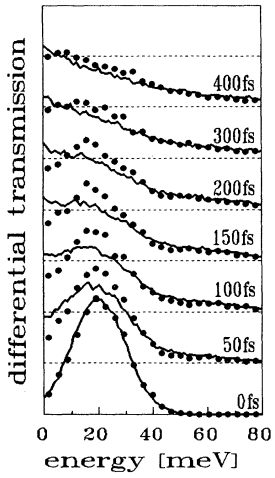

FIG. 4. Differential transmission vs excess photon energy, based on Fig. 3. The distance between the horizontal grid lines is 0.03.

rather than the hole distribution, while the MD spectra are strongly affected by the hole distribution (a small nonthermal peak in the MD spectra at 400 fs is due to nonthermal holes).

The thermalization would be even slower for the 2D plasma of finite thickness. A comparison of Figs. 1 and 3 shows this effect for the MC model. In the MD model, the finite thickness of the plasma[19] would slow down the thermalization due to the elimination of the divergency of the pair Coulomb forces at small intercarrier distance. Thus our MD model safely predicts at least four times longer (400 fs) thermalization of the nonthermal peak than the observed one.[1]

What is the origin of the differences between the MC and MD results? MD approximates quantum dynamics by a classical many-body dynamics. In the 3D case,[20] MD relies on the fact that classical dynamics yields the exact quantum differential cross section for unscreened Coulomb scattering between two carrier plane waves (neglecting exchange). The scattering of one carrier from others is correctly modeled by classical dynamics, as long as the positions of other carriers are uncorrelated so that individual scattering amplitudes add incoherently. In the 2D case, the exact quantum calculation for 2D electron–ionized-impurity scattering[27] gives a differential cross section that can be rewritten (see the remark later on) in our notation for e-h scattering as

$$\sigma(\theta) = \frac{G}{g}\frac{\tanh(\pi G)}{\sin^2\frac{\theta}{2}} \quad , \quad G = \frac{\mu e^2}{4\pi K g \hbar^2} \quad . \tag{13}$$

Generally, this result differs from the classical cross section $\sigma_{\rm cl}(\theta) = G/(g\,\sin^2\frac{\theta}{2})$, which follows from (13) when $\tanh(\pi G) \to 1$, i.e., when $\pi G \gg 1$[27]. We estimate the ratio $\sigma_{\rm cl}/\sigma$ for typical k and k_0 from the initial nonthermal distribution ($k = k_0 = 1.85 \times 10^8$ m^{-1}). Maximum values of $\sigma_{\rm cl}/\sigma$, found for $\mathbf{k}$ antiparallel to $\mathbf{k}_0$ (for $g = 3.7 \times 10^8$ m^{-1}), are 1.26, 1.06, and 1.00 for e-e, e-h, and h-h scattering, respectively. This implies that in our 2D case the MD simulation works well especially for h-h scattering, with e-e and e-h scattering slightly overestimated.

A remark should be made on the derivation of (13). In Ref. 27 the exact (partial wave) scattering cross section is derived for 2D electron–ionized-impurity scattering. This cross section can be transformed into (13) using the replacement $v_e \to |\,\mathbf{v}_e - \mathbf{v}_h\,|$ and $m_e \to m_e m_h/(m_e + m_h)$, where v and m are the carrier velocity and carrier effective mass. This transformation is exact as shown in Ref. 28, where the partial wave cross section is derived (in the 3D case) for two colliding particles of different effective masses. The only difference compared to the case $m_h \to \infty$ is the use of $m_e m_h/(m_e + m_h)$ and $|\,\mathbf{v}_e - \mathbf{v}_h\,|$ instead of m_e and v_e, respectively.

Now we wish to assess the validity of the Born approximation in our MC simulation. Expression (13) provides the unscreened Born approximation $\sigma_B(\theta) = \pi G^2/(g\,\sin^2\frac{\theta}{2})$, when $\tanh(\pi G) \to \pi G$, i.e., when $\pi G \ll 1$.[27] A similar estimation as for $\sigma_{\rm cl}/\sigma$ now yields $\sigma_B/\sigma =$ 1.36, 1.91, and 7.07. Due to low carrier density it can be shown that this estimation is reasonably good also for the screened Born approximation in our MC simulation. The screened Born approximation[29]

$$\sigma_B(\theta) = \frac{\pi G^2}{g\,\sin^2\frac{\theta}{2}}\left(1 + \frac{Q_{\rm sc}}{g\,\sin\frac{\theta}{2}}\right)^{-2} \tag{14}$$

(written assuming a δ-shaped envelope function) is only about 1–1.21 times smaller than the unscreened σ_B, when $\sin\frac{\theta}{2} > 10Q_{\rm sc}/g$. Typical $Q_{\rm sc}/g$ for the initial carrier distributions are $\sim 1/300$ for e-e scattering ($Q_{\rm sc} \approx 1.25 \times 10^6$ m^{-1}) and $\sim 1/40$ for e-h and h-h scattering ($Q_{\rm sc} \approx 9.4 \times 10^6$ m^{-1}). The range of θ values determined by $\sin\frac{\theta}{2} > 10Q_{\rm sc}/g$ is quite large and contains scattering angles substantially contributing to the thermalization (artifical prohibition of these angles decelerates the thermalization several times). In this interval of scattering angles the screened σ_B can be approximated by the unscreened σ_B with an error of less than 21%, which is much smaller than the estimated difference between σ_B and σ (91% for e-h scattering, and 607% for h-h scattering). Thus our estimate of the unscreened σ_B/σ enables us to conclude safely that the Born approximation in our MC simulation overestimates the exact quantum cross section. The overestimation is large especially for h-h scattering.

To manifest this overestimation more clearly, Fig. 5 shows the electron thermalization due to e-e scattering and the hole thermalization due to h-h scattering. The hole thermalization is ten times faster in the MC simulation than in the MD simulation and this difference agrees reasonably with the difference between σ_B/σ and $\sigma_{\rm cl}/\sigma$ estimated for h-h scattering. As for the electron thermalization, the difference between the MC and MD results is much less pronounced than for the hole thermalization, because for e-e scattering the difference between σ_B/σ and $\sigma_{\rm cl}/\sigma$ is small. The remaining differences (the thermalization in the MD is slower than expected from the differences between $\sigma_{\rm cl}/\sigma$ and σ_B/σ) are mainly due to the following fact.[30] In the MC simulation the thermal-

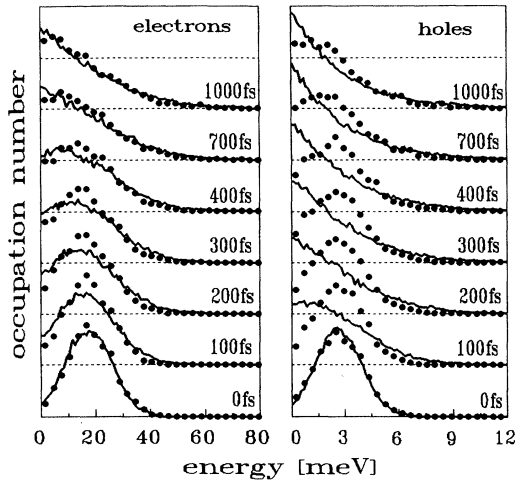

FIG. 5. The same material as in Fig. 3, except that now the simulation of electron (hole) dynamics ignores the presence of holes (electrons). Phonon scattering is ignored as well.

ization occurs through isolated binary collisions. These include also very frequent "small angle" collisions with classical impact parameter much larger than the mean interparticle distance. There is no place for this type of collisions in the MD, where the Coulomb forces from very distant scatterers tend to add vectorially to zero.

In contrast to our 2D study, in the 3D case[17] the relaxation of the nonthermal energy distribution is usually faster in the MD simulation than in the MC simulation. The faster thermalization in the 3D MD simulation is due to dynamic screening of carrier-carrier interactions and due to initial broadening of the nonthermal distribution during the very first (yet incompleted) carrier-carrier collisions.[31] In the MD simulation the latter effect is overestimated due to the pointlike nature of the simulated particles,[31] while it is not present in the MC simulation where carrier-carrier collisions are treated as instantaneous events. It certainly plays a role also in our 2D MD simulation, but its contribution to the initial broadening of the energy distribution has to be much less significant than the thermalizing effect of overestimated scattering cross sections in our 2D MC simulation.

IV. SUMMARY AND CONCLUDING REMARKS

We have reexamined the derivation of 2D carrier-carrier scattering in quantum wells. The carrier-carrier scattering rates are four times smaller than those derived previously.[8,9,12,13] Exchange is included within a multisubband model.

MC simulation with revised carrier-carrier scattering has been used to study the thermalization of a low-density 2D e-h plasma, excited into the lowest subband of an intrinsic GaAs quantum well. MC results (Fig. 2) predict that the initial nonthermal peak in the transmission spectra disappears later than at 200 fs and the thermalization is completed at 400 fs. This is in disagreement with experiment, where the corresponding time constants are 100 fs and 200 fs. The agreement with experiment found in previous MC simulations[6,7,9] is due to four-times-overestimated carrier-carrier scattering rates. The same holds about a recent study[10] of the hole relaxation in doped quantum wells.

The plasma thermalization has also been simulated by classical MD simulation. MD shows much slower thermalization than the MC simulation (Figs. 3, 4, and 5), because the classical differential cross section for carrier-carrier scattering is close to the exact quantum result (13), while the Born approximation overestimates this exact result. The initial nonthermal peak disappears in the MD simulation later than at 400 fs (Fig. 4),which is far from the experimentally observed value of 100 fs.[1]

We conclude that there is up to now to our knowledge, no quantitative theoretical confirmation that the 200 fs thermalization of the 2D e-h plasma excited in an intrinsic GaAs quantum well by a short laser pulse[1,3] is due to carrier-carrier scattering. Our conclusion is in contrast with previous MC simulations, criticized in this paper. Despite this criticism we believe that these simulations represent an important step towards the understanding of the ultrafast 2D carrier thermalization. For completeness we mention also the MC study of Ref. 32. The authors of that reference found a good agreement with the measured 200 fs thermalization[1] assuming that (i) photoexcited holes can be ignored, (ii) electron background density is 6×10^{10} cm^{-2}, and (iii) the screening can be described by time-independent Debye screening due to equilibrium background electrons. Assumption (iii) strongly underestimates the initial e-e scattering rate, because the Debye screening vector is about 25 times larger than our initial $Q_{sc} \approx 1.25 \times 10^6$ m^{-1}. This underestimation tends to be balanced by assumption (ii) and the background density is chosen to fit the experiment. Since the expected actual background density[7] is 30 times lower than 6×10^{10} cm^{-2} and the photoexcited holes cannot be neglected (Figs. 1–5), this MC model likely cannot explain the experiment.[1] In Ref. 32 the 2D e-e scattering rate was not published in the final analytical form (5), so we cannot compare (5) with that work.

Empirical modeling of laser excitation[9] instead of our instantaneous photoexcitation would not change the conclusions of our paper. Recently,[33] the modeling of coherent interaction between carriers and laser pulse has been coupled with the MC simulation of 3D plasma thermalization. Perhaps a similar model of coherent interaction is necessary to interpret the 2D plasma thermalization,[1] but it should not be coupled with the MC simulation, which treats the 2D carrier-carrier scattering using the Born approximation.

Our conclusion on the invalidity of the Born approximation in the 2D MC simulation is restricted to low e-h pair densities (close to 2×10^{10} cm^{-2} or lower) and to photoexcitation near the band edge.[1,3] This conclusion may no longer be valid at much higher carrier densities[2] and/or at much higher excitation energies. It is also not applicable to 3D carrier dynamics (for example, in the 3D case $\sigma_B = \sigma_{cl} = \sigma$ for the unscreened Coulomb interaction).

It is tempting to speculate that the inclusion of dy-

namic screening into our 2D MC model could provide the necessary acceleration of the thermalization compared to the experiment. At the same time the dynamically screened scattering cross section would become closer to the unscreened one than the statically screened cross section. Thus the breakdown of the Born approximation would be manifested even more convincingly than for static screening, because the unscreened Born approximation evidently breaks down. Due to this breakdown such an agreement of the MC simulation with experiment would be misleading. However, the results obtained using quasidynamic screening [Fig. 2(a)] are close to the results obtained using static screening [Fig. 2(b)], and this suggests that the effect of dynamic screening is not important in our low-density case.

It seems that two problems have to be solved in order to understand the pump-probe spectra[1,3] quantitatively. First, one needs a MC simulation which treats carrier-carrier scattering beyond the Born approximation. Second, one needs to separate the actual relaxation to a Maxwellian distribution from the merging of the free carrier bleaching into the background of the exciton peak.[1,3] It is possible that dynamic change of the exciton peak causes the apparent thermalization (as measured from absorption) to be faster than the actual thermalization of the individual electron and hole distributions.

[1] W.H. Knox, C. Hirliman, D.A.B. Miller, J. Shah, D.S. Chemla, and C.V. Shank, Phys. Rev. Lett. **56**, 1191 (1986).

[2] W.H. Knox, D.S. Chemla, G. Livescu, J.E. Cunningham, and J.E. Henry, Phys. Rev. Lett. **61**, 1290 (1988).

[3] J.B. Stark, W.H. Knox, and D.S. Chemla, Phys. Rev. Lett. **68**, 3080 (1992).

[4] S.M. Goodnick and P. Lugli, Appl. Phys. Lett. **51**, 584 (1987).

[5] S.M. Goodnick and P. Lugli, Solid State Electron. **31**, 463 (1988).

[6] S.M. Goodnick and P. Lugli, Phys. Rev. B **38**, 10 135 (1989).

[7] S.M. Goodnick, P. Lugli, W.H. Knox, and D.S. Chemla, Solid State Electron. **32**, 1737 (1989).

[8] S.M. Goodnick and P. Lugli, Phys. Rev. B **37**, 2578 (1988).

[9] S.M. Goodnick and P. Lugli, in *Hot Carriers in Semiconductor Nanostructures*, edited by J. Shah (Academic, New York, 1992), Chap. 31, p. 191.

[10] A. Tomita, J. Shah, J.E. Cunningham, S.M. Goodnick, P. Lugli, and S.L. Chuang, Phys. Rev. B **48**, 5708 (1993).

[11] P.W. Blom, J. Haverkort, P.J. van Hall, and J.H. Wolter, Appl. Phys. Lett. **62**, 1490 (1993).

[12] M. Moško and A. Mošková, Phys. Rev. B **44**, 10 794 (1991).

[13] A. Mošková and M. Moško, Phys. Rev. B **49**, 7443 (1994). The expression for *e-h* scattering rate involves a mistake. To have a valid expression, $\mathbf{k}-\mathbf{k}_0$ has to be replaced by $\mathbf{g}$ in the formulas (8) and (9). This mistake was not involved in the numerical simulations. The same problem appears in Ref. 14.

[14] M. Moško and A. Mošková, Semicond. Sci. Technol. **9**, 478 (1994).

[15] V. Cambel and M. Moško, Semicond. Sci. Technol. **9**, 474 (1994).

[16] N. Takenaka, M. Inoue, and Y. Inuishi, J. Phys. Soc. Jpn. **47**, 861 (1979).

[17] L. Rota, P. Lugli, T. Elsaesser, and J. Shah, Phys. Rev. B **47**, 4226 (1993).

[18] M. Moško and V. Cambel, Phys. Rev. B **50**, 8864 (1994).

[19] R.P. Joshi, A.M. Kriman, M.J. Kann, and D.K. Ferry, Appl. Phys. Lett. **58**, 2369 (1991).

[20] M.G. Kane, K.W. Sun, and S.A. Lyon, Semicond. Sci. Technol. **9**, 697 (1994).

[21] V. Cambel and M. Moško, Semicond. Sci. Technol. **8**, 364 (1993).

[22] The finite step and the divergency of the pair Coulomb force at zero distance can cause numerical instability of the solution. Therefore, if accidentally two carriers become closer than a critical distance b, the force between them is approximated by its value at b [see R. Hockney and J. Eastwood, *Computer Simulation Using Particles* (McGraw-Hill, New York, 1981)]. For $\Delta t = 0.1$ fs we use $b = 1$ nm. We have a numerically stable simulation with a three-digit accuracy of the total energy conservation. Changes of the results were insignificant when the accuracy was increased using $\Delta t = 0.03$ fs and $b = 0.05$ nm, or decreased using $\Delta t = 0.5$ fs and $b = 2.5$ nm. Thus the most serious error — the wrong calculation of *e-h* interactions for $|\mathbf{r}_i - \mathbf{r}_j| < b$ — is negligible in our case.

[23] T. Yamada and D.K. Ferry, Phys. Rev. B **47**, 6416 (1993).

[24] We obtain the same simulation results for $N = 3200$ and 6400. The results are close to those obtained in Ref. 15 for $N = 28\,800$ with only 50 nearest neighbors considered in the calculation of $\mathbf{F}_i$.

[25] A similar procedure as in Ref. 18 shows us for each type of carriers separately that the initial radial distribution is close to the equilibrium one, i.e., that the effect of the relaxation in $\mathbf{r}$ space is unimportant.

[26] D.W. Snoke, Phys. Rev. B **47**, 13 346 (1993).

[27] F. Stern and W.E. Howard, Phys. Rev. **163**, 816 (1967).

[28] L. Schiff, *Quantum Mechanics* (McGraw-Hill, New York, 1955).

[29] The differential cross section (14) follows from the carrier-carrier scattering rate (Sec. II), rewritten in the standard form $\Gamma_{11}(\mathbf{k}) = \sum_{\mathbf{k}_0,s_0} f_1(\mathbf{k}_0)(\hbar g/\mu)\int_0^{2\pi} d\theta\ \sigma_B(\theta)$ for a "single-subband" model. When $m_h \to \infty$ and $Q_{sc} = 0$, σ_B is the same as the unscreened Born approximation for 2D electron-donor scattering (Ref. 27).

[30] A. Mošková and M. Moško (unpublished).

[31] M.G. Kane, K.W. Sun, and S.A. Lyon, Phys. Rev. B **50**, 7428 (1994).

[32] D.W. Bailey, M. Artaki, C.J. Stanton, and K. Hess, J. Appl. Phys. **62**, 4638 (1987).

[33] F. Rossi, S. Haas, and T. Kuhn, Semicond. Sci. Technol. **9**, 411 (1994).